Journal of Nepal Geological Society, 2006, Vol. 34, pp. 117–128

GIS-based modelling of landslide and debris flow hazard in mountainous terrain of Agra Khola watershed, central Nepal

***P. B. Thapa[1,2], T. Esaki[2], and B. N. Upreti[1]**
[1]*Department of Geology, Tri-Chandra Campus, Tribhuvan University, Kathmandu, Nepal*
[2]*Institute of Environmental Systems, Faculty of Engineering, Kyushu University, Fukuoka, Japan*
*(*Email: geoscithapa@yahoo.com)*

ABSTRACT

A comprehensive GIS-based analytical approach was followed to derive a spatial database of landslides and debris flows in the Agra Khola watershed of central Nepal which suffered from the hydrological disaster of 1993. For this purpose, the landslides and debris flows occurring in that area between 1993 and 2006 were delineated. From the database, the influence of geological and geomorphic variables was quantified and a spatial prediction model for landslide and debris flow hazard was worked out. In this process, quantitative statistical analysis (bivariate, multivariate) was applied to predict elements or observations between stable and unstable zones. The predicted results were classified into various hazard levels in a hazard map and were validated by comparing it with the landslide and debris flow distribution map of the Agra Khola watershed. Also the GIS-based hazard prediction model has objectivity in the procedure and reproducibility of the results in the mountainous terrains.

INTRODUCTION

Landslides and debris flows are the most damaging natural disasters in a mountainous terrain such as the Himalayas and they are also widespread worldwide (Rowbotham and Dudycha 1998; Guzzetti et al. 1999). Consequently, they create major ecological and environmental problems in a larger geographical area and require considerable financial costs for their control and mitigation.

In the mountains, there are a wide variety of slope movements such as soil slips, deep-seated slides, mudflows, debris flows, and rock falls (Varnes 1978; Hutchinson 1988; Cruden and Varnes 1996; Hungr et al. 2001). Different methods and techniques for evaluating landslide occurrence have been developed and proposed worldwide (Hansen 1984; Varnes 1984; Crozier 1995). They can be grouped into the inventory, qualitative, statistical, and deterministic approaches (Soeters and van Westen 1996; van Westen et al. 1997; Atkinson and Massari 1998). Landslide inventory mapping is the most straight-forward initial approach to any study of regional landslide hazard and is the basis of most susceptibility mapping techniques (Soeters and van Westen 1996). In qualitative approaches, several maps representing the spatial distribution of factors that may influence the occurrence of landslides are combined to produce a susceptibility map, using subjective decision rules, based on the experience of the geoscientists involved (Anbalagan 1992; Pachauri and Pant 1992; Sarkar et al. 1995). In statistical approaches, statistical analysis is used to determine the relation between landslide susceptibility and a number of factors that are considered to have an influence on landslide occurrence. This relation is then applied to map landslide susceptibility (Yin and Yan 1988; Carrara et al. 1991; Dhakal et al. 1999). Deterministic approaches are based on slope stability analyses and are applicable only when the ground conditions are fairly uniform across the study area, the landslide types are known, and they are relatively easy to analyse. Despite the methodological and technical differences, most proposed methods consider that geomorphic and geological conditions of future landslides should be similar to those conditions that led to past and present slope movements, together with the identification and mapping of the conditioning or preparatory factors of slope instability, and are the keys in predicting future landslides (Carrara et al. 1998, 1999).

Quantitative statistical analysis of landslides and debris flows is carried out when geo-material data (mechanical properties, water saturation, etc.) are difficult to obtain over large areas (Terlien et al. 1995). Hazard modelling in the Agra Khola watershed of central Nepal was assessed quantitatively based on the relationship between the potential for landsliding (dependent variable) and a set of intrinsic properties (independent variables) using a geographic information system (GIS).

STUDY AREA

The study area (Fig. 1) lies in central Nepal (latitude: 27°36'–27°45' N, longitude: 84°58'–85°72'E). The Agra Khola is the main stem river and the altitude of its watershed ranges from 600 to 2480 m with a total area of 111.8 km^2.

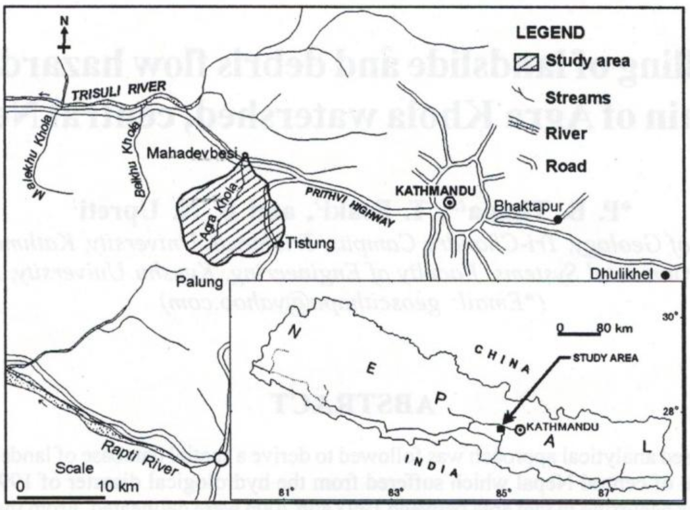

Fig. 1: Location of the study area

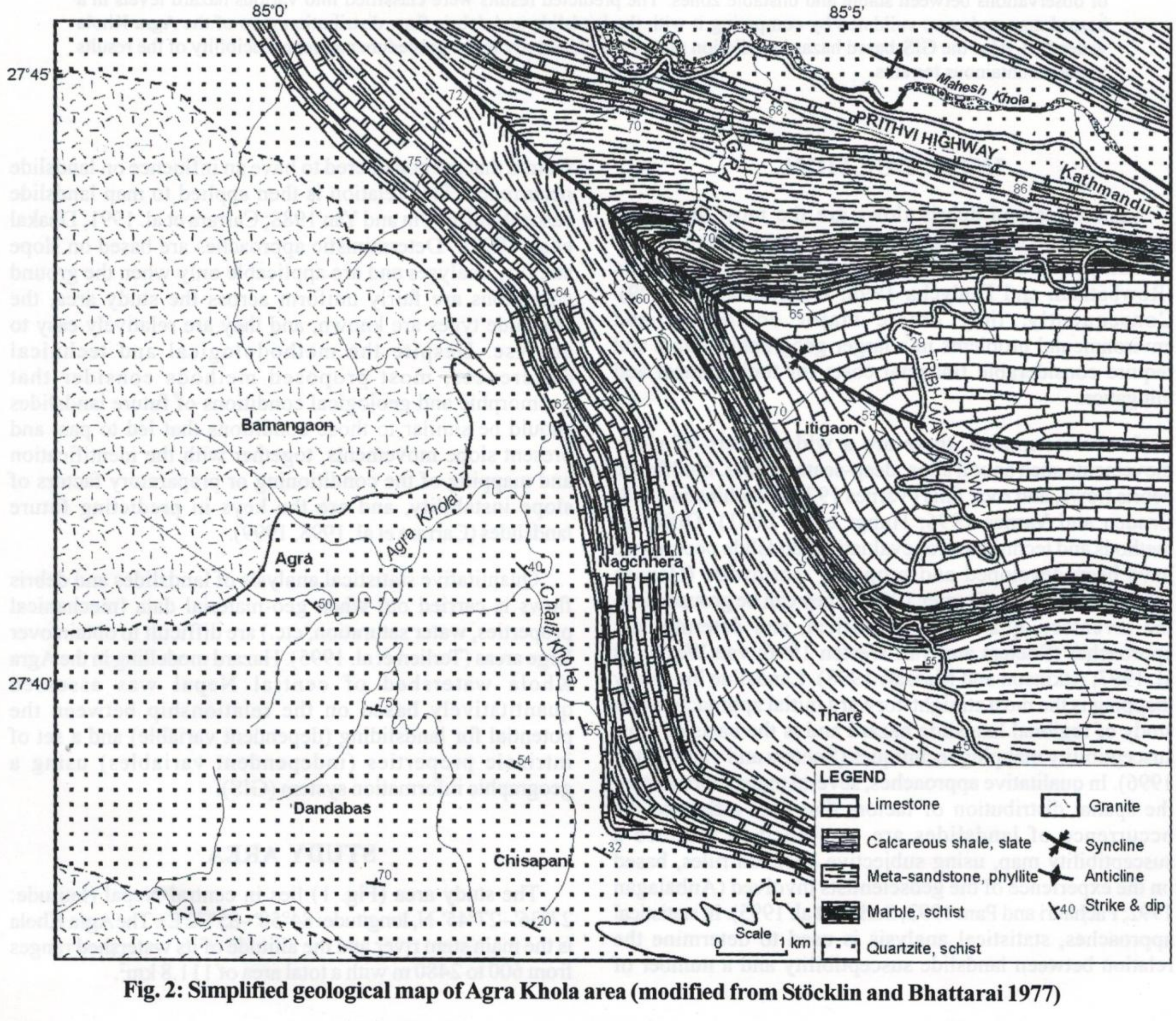

Fig. 2: Simplified geological map of Agra Khola area (modified from Stöcklin and Bhattarai 1977)

Table 1: GIS data layers of the study area

Classification	Coverage	Spatial data	Attribute data
Geological hazard	Landslide	Polygon	Nominal
Damageable object	Building, Road	Point, polyline	Nominal
Basic maps	Topographic map	Point, polyline	Nominal, interval
	Geological map	Polygon	Nominal
	Engineering geol. map	Polygon	Nominal
	Land use	Polygon	Nominal
Hydrologic data	Precipitation	Point, polyline	Nominal, interval

The area exhibits highly dissected and rugged topography in the south whereas it is relatively smooth in the north. The hill slopes are covered mainly by residual soils and colluvium. The residual soils occupy much of the area and have variable depths and aerial extents. The colluvium is scattered on foothills and also occurs as ribbon-like deposits filling drainage courses. Small alluvial deposits occur along the river valleys but they are generally confined to fans developed below the colluvial deposits. The regolith or mantle of weathered rock occurs over most of the rocky area.

The study area consists predominantly of Precambrian to Palaeozoic low- to medium-grade metamorphic rocks, such as metasandstones, slates, phyllites, marbles, quartzites, and schists (Stöcklin and Bhattarai 1977; Stöcklin 1980). Granite is intruded in the south-western part of the area whereas limestone crops out in the eastern region. The strata in the southern belt dip 32–85° due northeast to north and in the northern belt they dip 45–81° due southwest. The closure of the Mahabharat Synclinorium is observed in the study area (Fig. 2).

The high-intensity rainfall of 19–21 July 1993 triggered off numerous rock- and soil slides in the Agra Khola watershed. During that event, the nearest rain gauge station at Tistung recorded a 24-hour maximum precipitation of 540 mm (DHM 1993). Due to that extreme event, major slope failures occurred in the uppermost catchment of the study area causing 42 casualties (Thapa and Dhital 2000). Large deep-seated rockslides were confined to the north-facing dip slopes, whereas shallow slides were observed on counter dip slopes and in the area occupied by granite. A number of landslides were also seen in the middle reaches of the watershed with huge debris deposition in the middle sections of rivers. The Prithvi Highway lost its four-span bridge over the Agra Khola on the early morning of 20 July 1993. The segments of the Tribhuvan Highway within the Agra Khola watershed were also severely damaged.

SPATIAL DATABASE AND GIS ANALYSIS

A landslide inventory may represent a single event or multiple events (Chacón et al. 2006). The landslide inventory of the Agra Khola watershed (Fig. 3) included the instabilities occurring in that area between 1993 and 2006. It was prepared from the existing topographic maps, interpretation of aerial photographs, and detailed field survey.

Data acquisition and database creation

A triangulated irregular network (TIN) was created from the 1:25,000 scale digital topographic maps and a digital elevation model (DEM) with a 10 m x 10 m grid size was derived from it (Fig. 4). The DEM was utilised to produce the slope angle and slope aspect overlays. Also, the drainage lines were extracted from the DEM and ranked into five orders using Strahler's classification.

The vector layers of lithology, land use, and engineering geology were prepared (Fig. 4) from the available maps and field survey. Soil depths were estimated in the field and classified into thin (1–3 m) and thick (more than 3 m) types. The rock slope or soil cover with a thickness of less than 1 m was included in the rocky terrain and categorised into a low rock mass strength (LRMS), medium rock mass strength (MRMS), and high rock mass strength (HRMS). The rock mass strength classification was based on the measurement of intact rock and rock mass properties. A land use layer was prepared from the topographic maps and field survey, and was classified into forestland, shrub land, grassland, cultivated land, debris, and water bodies.

A database was created by inputting and linking spatial as well as attribute data (Fig. 4). The basic data layers produced from the GIS include landslide inventory, factors responsible for causing slope failures, and damageable objects (Table 1). In establishing the reclassification criteria for continuous variables, a compromise was made between the need to have a limited number of classes and a sufficiently wide range of original categories in each class (Fig. 5).

In a GIS overlay operation, the layers with a common, registered map base were joined on the basis of their spatial distribution (Thapa and Esaki 2006). In this process, an overlay function creates composite maps by combining diverse datasets from raster and vector models (Burrough 1986).

Attribute assigning

The landslide map was vectorised at the scale of 1:25,000 with attributes of typology, activity, morphometric parameters, and slope properties. To each landslide feature was assigned a unique ID and a link to the landslide database was established allowing the direct production of layers reflecting any variable from the database. Thus, a digitised map of landslide points and boundaries was produced. The last attribute database, but the most important one, is the transferred attribute database consisting of the variables responsible for the slope failure (Table 2).

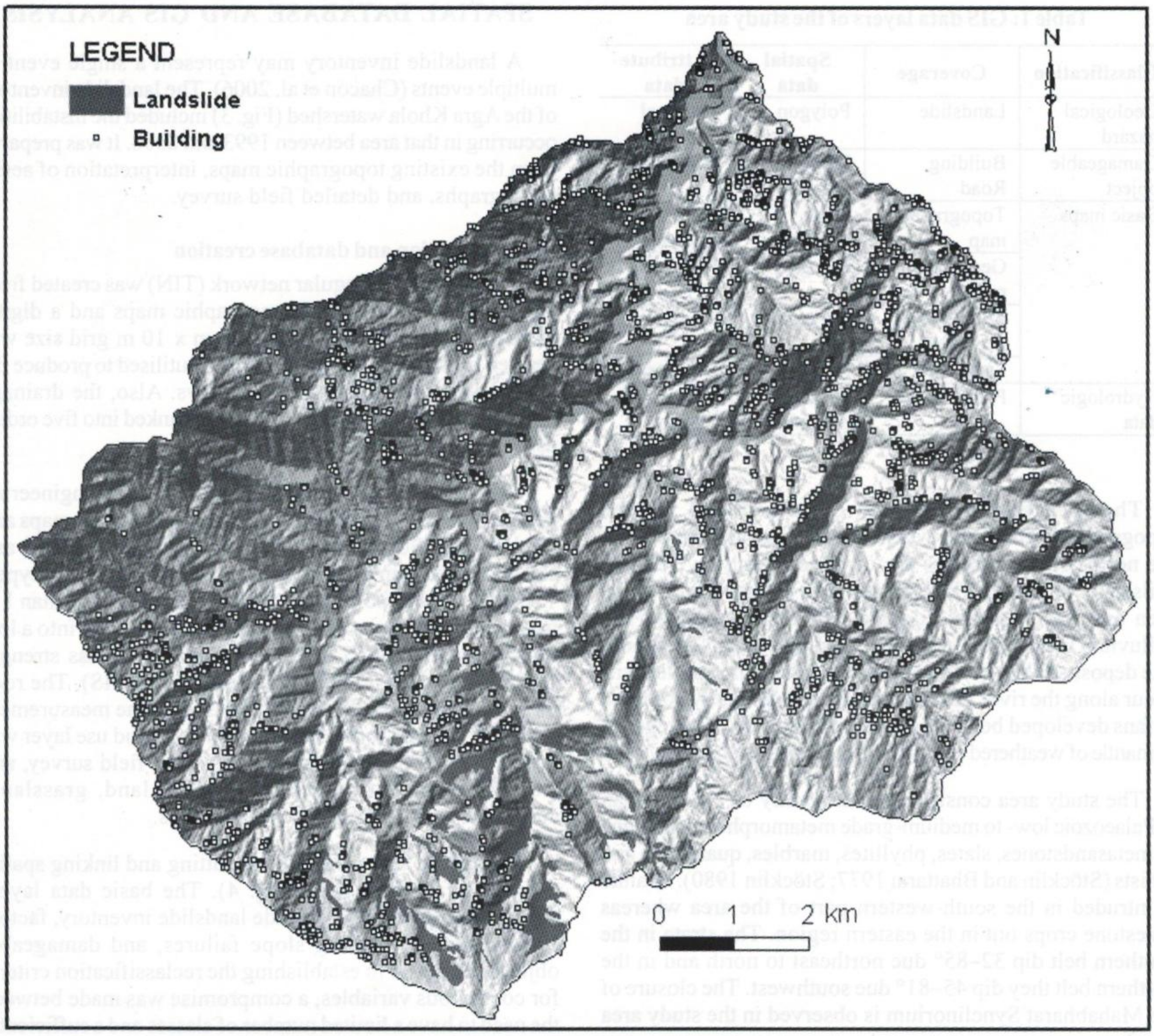

Fig. 3: Landslide inventory map of the Agra Khola watershed (draped on hill shade)

Table 2: The nature and ranges of transferred attribute database

Variable	Definition	Nature	Range
Lithology	Outcropping material	Nominal	–
Dist-drainage	Distance from drainage	Float	0–20 m
Slope aspect	Slope face	Float	-1–359
Slope angle	Natural slope	Float	0º–84º
Land use	Land cover	Nominal	–
Engineering geology	Surficial cover	Nominal	
Elevation	Height	Float	600–2480 m

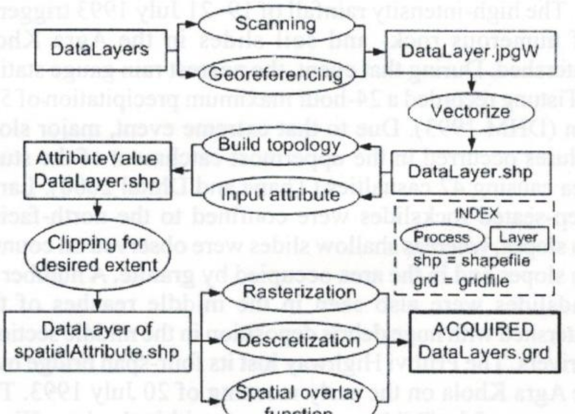

Fig. 4: General GIS procedure for data acquisition and database creation

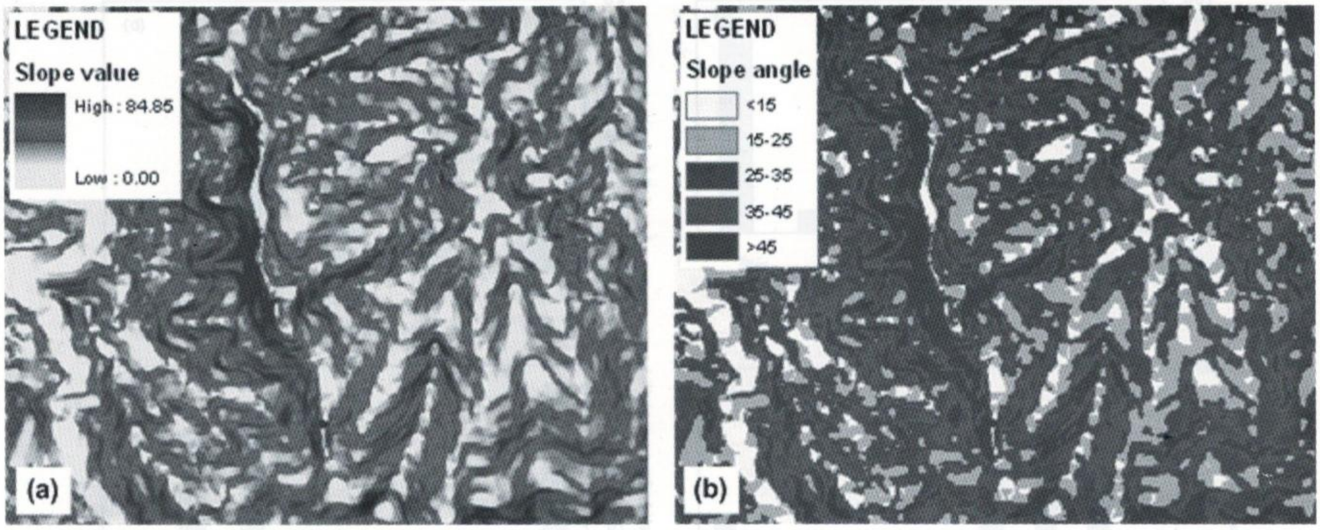

Fig. 5: Conversion of variable from continuous to discrete (e.g. reclassification of slope map)

The landslide inventory map was converted to a 10 m x 10 m grid file. Each cell was assigned "0" if the landslide was absent or "1" if the landslide was present and a "no data" code was assigned if the cell was outside the study area. The landslide grid file and causative variable grid file were logically compared to ensure that they covered a common area and then combined together in the centre of each cell (Fig. 6). Thus, all the attributes extracted were stored in a point base map file indicating the presence or absence of an instability.

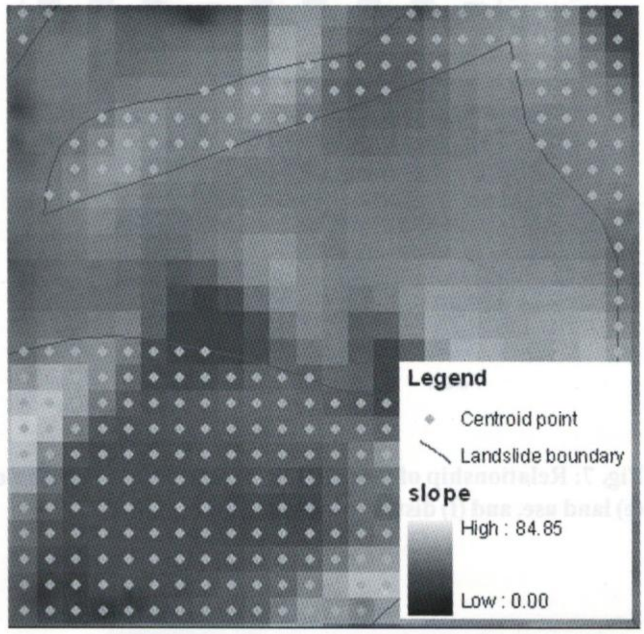

Fig. 6: Acquisition of attribute values from raster layers at centroids of landslide features

Analysis of variables

Univariate probability analysis was carried out to examine the physical variables contributing to the initiation of landslides. Numerous slope failures are observed in the quartzite and schist unit, which is due to a steep hill slope and favourable orientation of foliation in the direction of slope face (Figs. 7a, 8). Soil slides are most frequent on slope angles of 27° within the slope range of 25°–35° (Fig. 7b). But, when slopes exceed 45°, a sharp decrease in the landslide frequency is observed and the slope failures are more apt to fail as rockslides. Similarly, there are more landslides on north-facing slopes than on south-facing ones (Fig. 7c). Engineering geological analysis showed that most of the slides are on weathered rock slopes or in the area covered by thin soil resting on bedrock (Figs. 7d, 9). Cultivated land, grassland, and shrub land have comparatively more slope failures (Fig. 7e). The adjacent first-order drainage contributed more to slope failures than the distant streams of higher orders (Fig. 7f).

The debris flows (Fig. 10) are most common in the channel bed with a gradient not exceeding 20°. The debris flow paths were identified from the DEM by finding the direction of flow and the steepest descent, or a maximum drop from each cell (Thapa 2005). In this process, two different flow paths were seen: an ordinary path was following the stream channel and an anomalous path was passing over the obstacles or embankments.

QUANTITATIVE HAZARD MODELLING

Quantitative hazard modelling computes the likelihood of landslide occurrence from statistical relationships between past instabilities of a given type and spatial data layers of causative variables. For the past two decades, tools and techniques of quantitative landslide hazard modelling have advanced considerably (e.g. Carrara et al. 1999; Montgomery

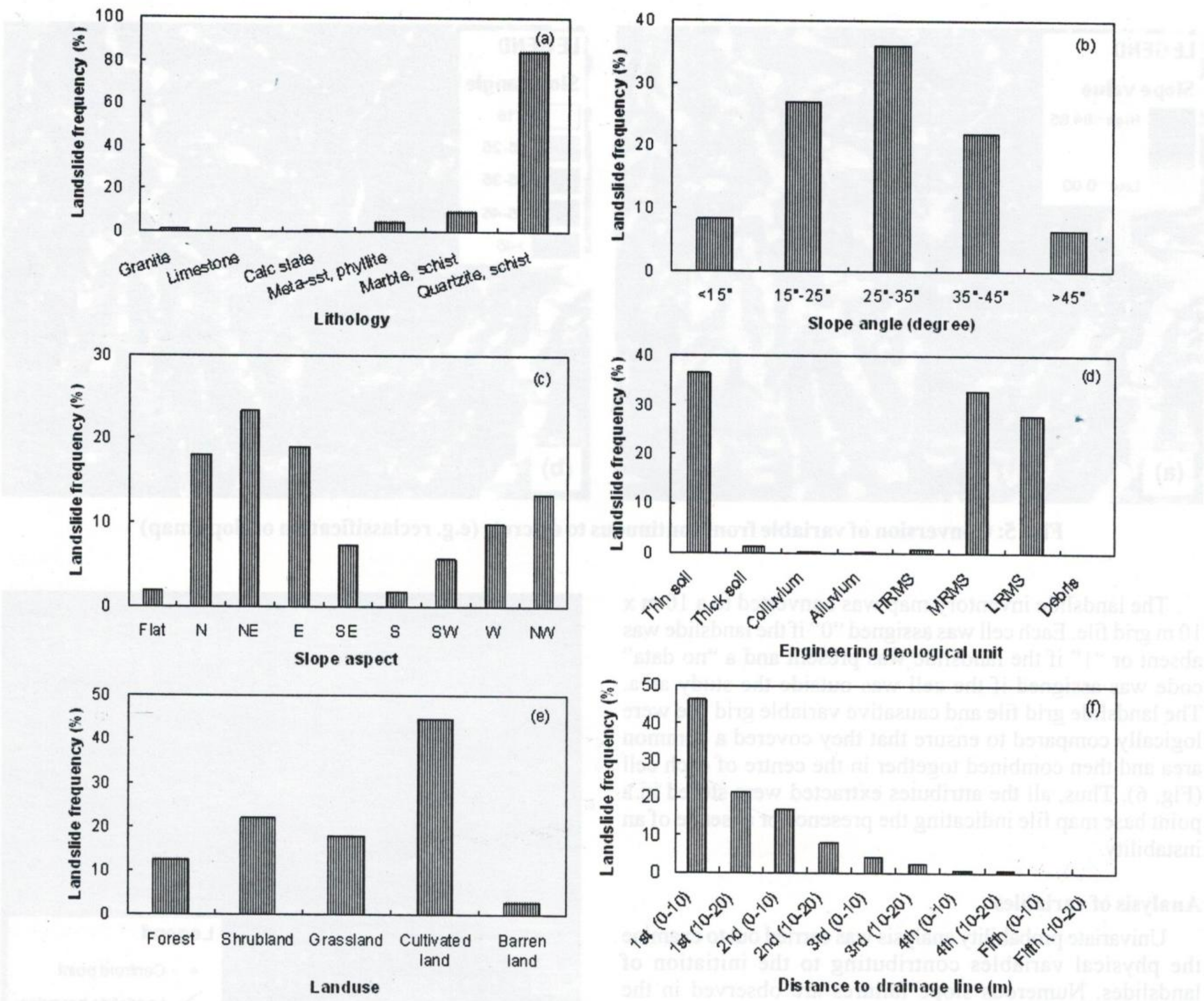

Fig. 7: Relationship of landslide frequency with: (a) lithology, (b) slope angle, (c) slope aspect, (d) engineering geology, (e) land use, and (f) distance to drainage

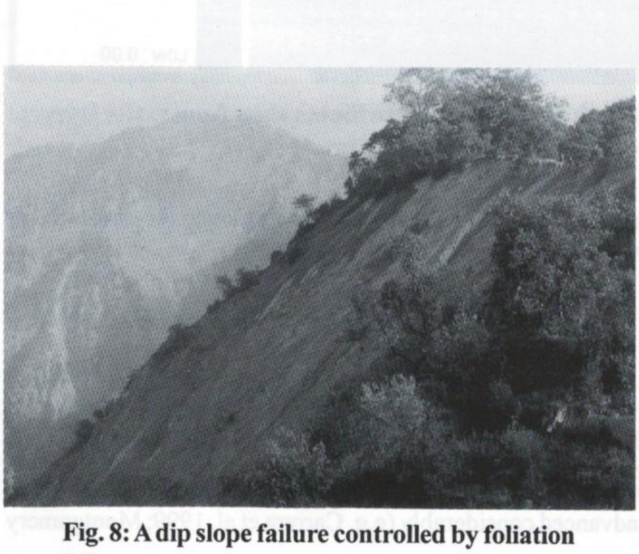

Fig. 8: A dip slope failure controlled by foliation

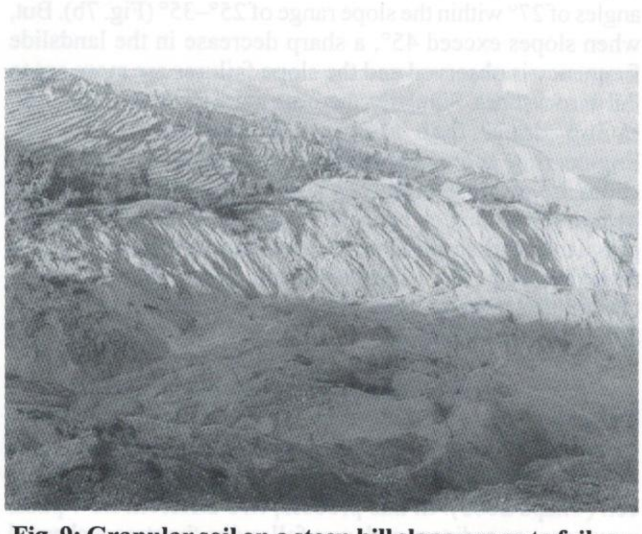

Fig. 9: Granular soil on a steep hill slope prone to failure

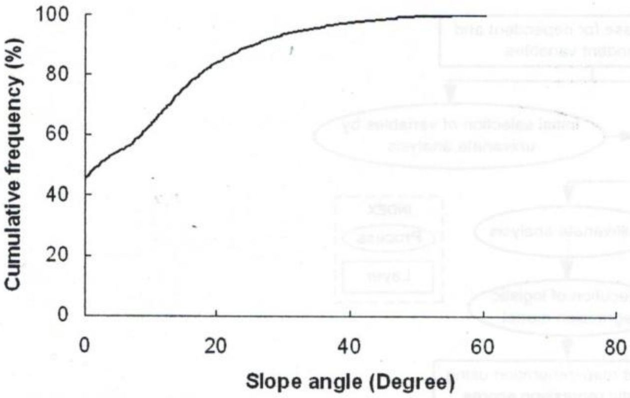

Fig. 10: Plot of cumulative frequency of debris deposition versus natural slope angle measured along the drainage networks derived from DEM

and Dietrich 1994; Mark and Ellen 1995). In these models, hazard levels are expressed in terms of mathematical functions such as a probability function. In such a model (Fig. 11), the optimum mapping units are selected based on univariate analysis whereas bivariate and multivariate analyses are used to compute the landslide hazard.

In the present study, the variables (i.e. elevation, slope angle, slope aspect, and drainage) were derived from the DEM as well as from the overlays of lithology, engineering geology, and land use. They were selected based on their influence on landslide occurrence and were ultimately converted to a matrix of causative variables. Grid and slope units were the mapping units of the model. Grids were acquired through the process of rasterisation and slope units were extracted from the DEM using Arc Hydro Tool of ESRI and Slope Unit Tool (Esaki et al. 2004).

Bivariate analysis and hazard map creation

Bivariate statistical analysis was carried out to generate statistically derived numerical weights (Equation 1) for all classes of the variable maps. The weights of the variables (Densclas) were calculated to compare the density of a variable class with the overall density (Densmap) in the parameter map of the whole catchment area (van Westen 1993). The analysis is carried out by 'crossing' a landslide map (dependent variable) with a certain independent variable map. The map 'crossing' results in a 'cross table', which is used to calculate the density of landslides per variable class. The landslide density per class is divided by the landslide density in the entire map.

$$Wi = \ln\left(\frac{Densclas}{Densmap}\right) = \ln \frac{Npix(SXi)\,/\,Npix(Xi)}{\sum_{i=1}^{n} Npix(SXi)\,/\,\sum_{i=1}^{n} Npix(Xi)} \qquad (1)$$

where Wi = the weight of certain variable class (e.g. slope class), $Npix(SXi)$ = Number of pixels with landslide within variable class Xi, and $Npix(Xi)$ = Number of pixels within variable class Xi.

The weighted thematic maps generated in this way are numerically added to produce a landslide susceptibility index (*LSI*) map (Equation 2).

$$LSI = Li + Eng + Elv + Sl + Sa + Dd + Lu \qquad (2)$$

where *Li, Eng, Elv, Sl, Sa, Dd* and *Lu* are derived weight maps of lithology, engineering geology, elevation, slope angle, slope aspect, distance to drainage, and land use respectively.

Multivariate analysis and hazard prediction

Due to the binary character of the response and some predictor variables, and the dubious normality of some of the variables, a logistic regression procedure was selected. The logistic regression model considers several physical variables that may affect probability and accepts both binary and scalar values as the independent variables, which allows for the use of variables that are not continuous or qualitatively derived. All input variables are grouped into a few meaningful classes. No subjective judgement is involved in the categorical data, such as lithology, engineering geology, and land use. For continuous variables, such as slope angle or elevation, the selection of the number of classes and class limits requires a significant amount of guess work guided by previous knowledge of the causal relationships between slope failures and instability factors (Guzzetti et al. 1999).

Using the overlay capabilities of GIS, the attribute data were georeferenced to the mapping units (viz. slope units). In this process an important step was the conversion of various nominal parameters (e.g. lithology, land use) to numeric values. This was done automatically through a dummy variable matrix (Fig. 12).

The regional GIS database was then exported to statistical software for analysis (SPSS 1997). The technique of logistic regression yields the coefficients for each variable and these coefficients serve as weights in an algorithm, which is used in the GIS database to produce a map depicting the probability of landslide occurrence. Quantitatively, the relationship between the occurrence and its dependency on several variables can be expressed as (Equation 3):

$$Pr(event) = 1/(1+e^{-Z}) \qquad (3)$$

where *Pr(event)* is the probability of an event occurring. In the present situation, Pr(event) is the estimated probability of landslide occurrence. As Z varies from $-\infty$ to $+\infty$, the probability varies from 0 to 1 on an S-shaped curve, where Z is the linear combination (Equation 4):

$$Z = B0 + B_1X_1 + B_2X_2 + \ldots + B_nX_n \qquad (4)$$

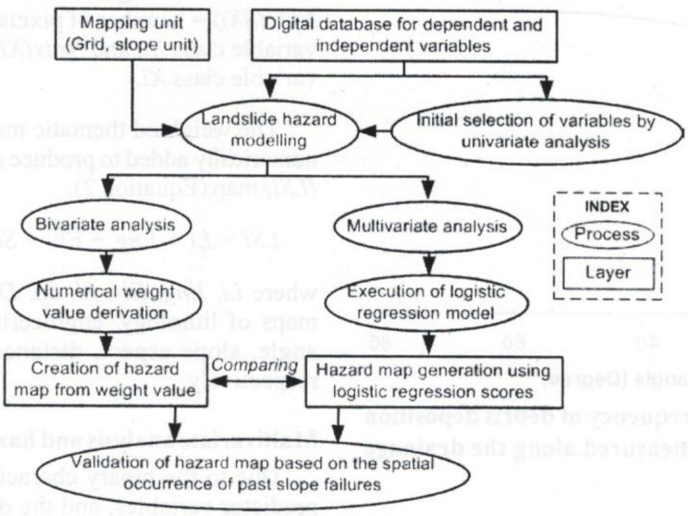

Fig. 11: Flowchart of landslide and debris flow hazard modelling

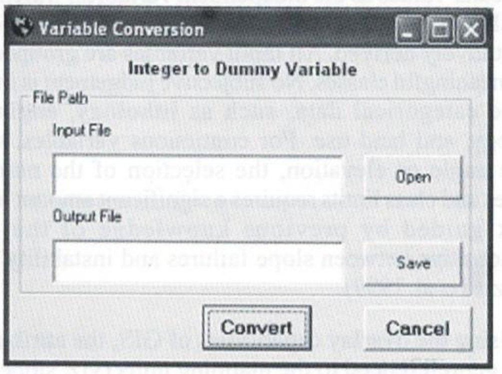

$$\begin{bmatrix} 21 & 0 & 0 & 11 & 23 & 0 \\ 0 & 76 & 56 & 0 & 15 & 0 \\ 0 & 0 & 87 & 0 & 98 & 7 \\ 98 & 0 & 0 & 90 & 0 & 0 \\ 34 & 41 & 33 & 0 & 0 & 0 \end{bmatrix} \rightarrow \begin{bmatrix} 1 & 0 & 0 & 1 & 1 & 0 \\ 0 & 1 & 1 & 0 & 1 & 0 \\ 0 & 0 & 1 & 0 & 1 & 1 \\ 1 & 0 & 0 & 1 & 0 & 0 \\ 1 & 1 & 1 & 0 & 0 & 0 \end{bmatrix}$$

Fig. 12: Example of matrix conversion from an integer variable to a dummy variable (Esaki et al. 2005)

where $B_i (i = 0, 1,..., n)$ is the coefficient estimated from the sample data, n is the number of independent variables (i.e. landslide-related physical parameters), and $X_i (i=1, 2,..., n)$ is the independent variable.

The coefficients for the final logistic regression are shown in Table 3. It should be noted that all the variables in the model are binary. For each variable, the last category is used as the default reference value, and the coefficient of that category is thus overridden.

The hazard map obtained from the multivariate analysis was based on the logistic regression scores. In logistic regression analysis, variables are evaluated for removal one by one if they do not contribute sufficiently to the regression equation. The likelihood-ratio test is used for determining whether variables should be added to the model. If the observed significance level is greater than the probability for remaining in the model (0.1 in this study), the variable is removed from the model and the model is recalculated to see if any other variables are eligible for removal. Two variables – elevation and distance to drainage, were removed from the model due to their lower significance values.

MODELLING RESULT AND VALIDATION

The final coefficients of logistic regression from SPSS were imported back to the GIS to prepare a hazard map (Table 3, Fig. 13). The landslide and debris flow hazard map generated from the analysis was classified into various hazard levels. Practically, there is no straightforward statistical rule to categorise continuous data automatically. Most of the researchers use their expert judgement along with available classification methods to develop class boundaries. The hazard is categorised into very low, low, medium, high, and very high levels using a natural junk-break method and overlaying the past landslide and debris flow map for the adjustment of class boundaries.

The predicted hazard map was validated following the methodology developed by a number of researchers (Carrara 1983; Brabb 1984; Yin and Yan 1988; Carrara et al. 1991; van Westen 1993; Carrara et al. 1995; Chung et al. 1995; Luzi and Pergalani 1996; Chung and Fabbri 2003; Remondo et al. 2003). The calculated and classified hazard levels (Fig. 13) are in

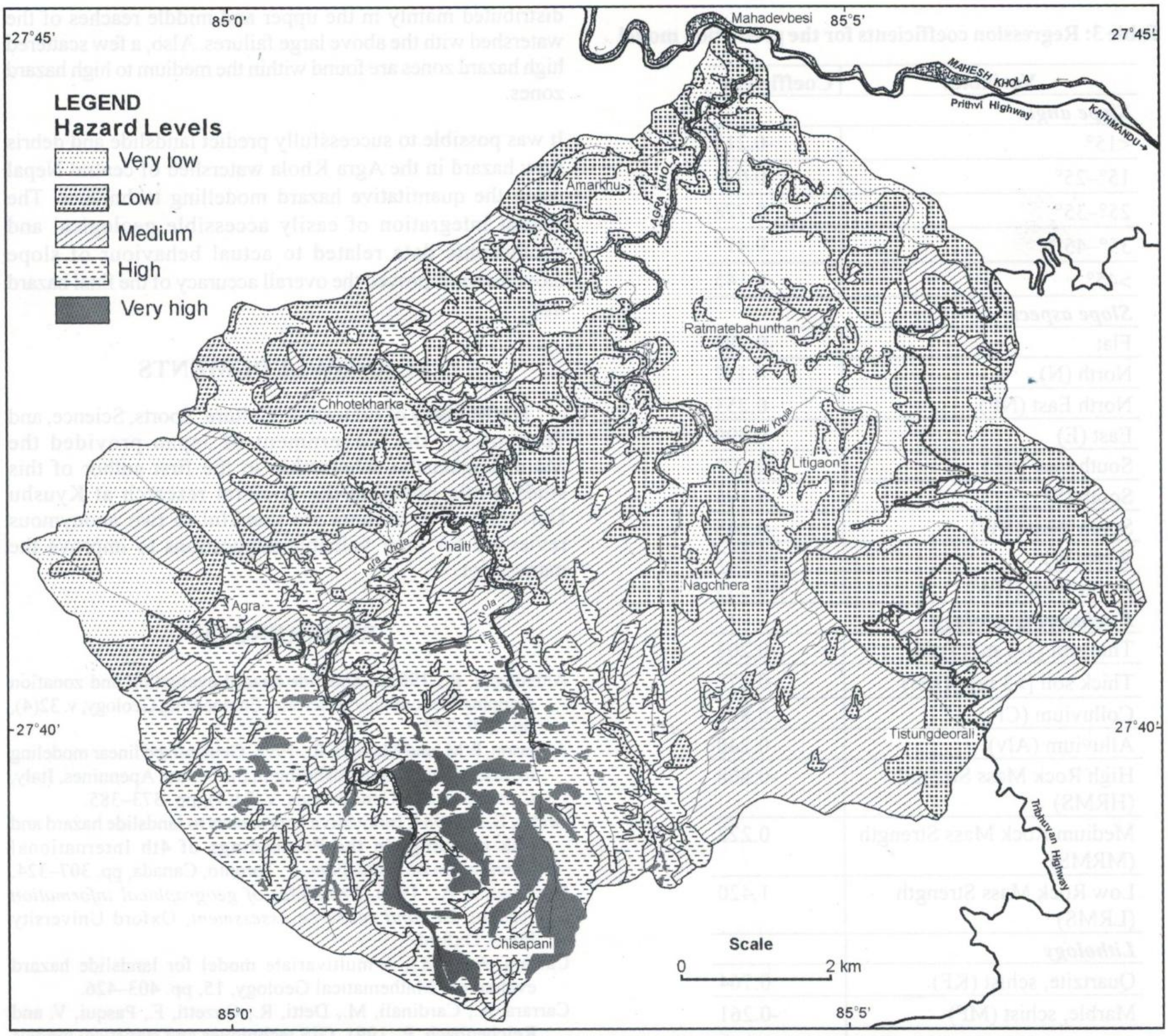

Fig. 13: Predicted landslide and debris flow hazard map of the Agra Khola watershed, central Nepal

good agreement with the distribution of landslides in the watershed (Fig. 14).

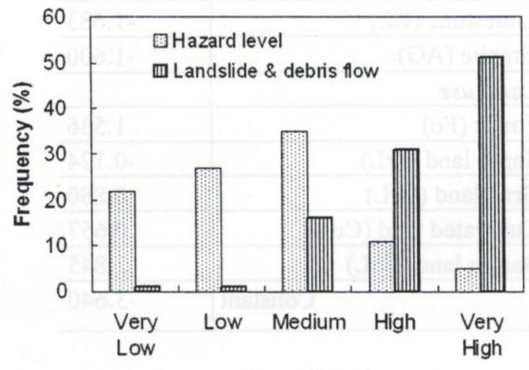

Fig. 14: Validation of hazard map using spatial occurrence of past landslide and debris flow events (Thapa et al. 2004)

CONCLUSIONS

The study showed that the slope angle, lithology, and foliation are the most influential parameters. The natural slope angle is the distinct pre-disposing factor for slope failures and a maximum number of failures are found on slopes of 27° within the slope range of 25°–35°. About 45% of debris is deposited on flat areas and on slopes of up to 20°. Large failures are confined to quartzites and schists, especially in the areas with thin soil cover on dip slopes or the slopes with day-lighting foliation. Very high hazard zones are also

Table 3: Regression coefficients for the prediction model

Variables	Coefficient
Slope angle	
<15°	-0.217
15°–25°	0.074
25°–35°	0.778
35°–45°	0.417
>45°	-0.145
Slope aspect	
Flat	-0.385
North (N)	0.117
North East (NE)	0.253
East (E)	0.590
South East (SE)	-0.177
South (S)	0.195
South West (SW)	-0.348
West (W)	-0.027
North West (NW)	0.333
Engineering geology	
Thin soil [1-3 m] (TnSl)	-0.203
Thick soil [>3 m] (TkSl)	-0.272
Colluvium (Clv)	-0.876
Alluvium (Alv)	0.240
High Rock Mass Strength (HRMS)	-0.868
Medium Rock Mass Strength (MRMS)	0.222
Low Rock Mass Strength (LRMS)	1.420
Lithology	
Quartzite, schist (KF)	0.764
Marble, schist (MF)	-0.261
Metasandstone, phyllite (TF)	-0.708
Calcareous slate (SF)	-1.516
Limestone (CL)	-1.683
Granite (AG)	-1.600
Land use	
Forest (Fo)	1.536
Shrub land (SrL)	-0.124
Grassland (GrL)	0.880
Cultivated land (CuL)	0.657
Barren land (BaL)	2.845
Constant	-3.640

distributed mainly in the upper and middle reaches of the watershed with the above large failures. Also, a few scattered high hazard zones are found within the medium to high hazard zones.

It was possible to successfully predict landslide and debris flow hazard in the Agra Khola watershed of central Nepal using the quantitative hazard modelling techniques. The spatial integration of easily accessible geological and geomorphic data related to actual behaviour of slope movements improved the overall accuracy of the final hazard map.

ACKNOWLEDGMENTS

The Ministry of Education, Culture, Sports, Science, and Technology, the Government of Japan provided the Monbukagakusho scholarship to the first author of this study while pursuing the doctoral research at Kyushu University. The authors are thankful to two anonymous reviewers for their valuable suggestions to improve the manuscript.

REFERENCES

Anbalagan, R., 1992, Landslide hazard evaluation and zonation mapping in mountainous terrain, Engineering Geology, v. 32(4), pp. 269–277.

Atkinson, P. M. and Massari, R., 1998, Generalized linear modeling of susceptibility to landsliding in the central Apennines, Italy, Computers and Geosciences, v. 24(4), pp. 373–385.

Brabb, E. E., 1984, Innovative approaches to landslide hazard and risk mapping, In the Proceedings of 4th International Symposium on Landslides, 1, Toronto, Canada, pp. 307–324.

Burrough P. A., 1986, *Principles of geographical information systems for land resource assessment*, Oxford University Press, Oxford.

Carrara, A., 1983, A multivariate model for landslide hazard evaluation, Mathematical Geology, 15, pp. 403–426.

Carrara, A., Cardinali, M., Detti, R., Guzetti, F., Pasqui, V. and Reichenbach, P., 1991, GIS techniques and statistical models in evaluating landslide hazard, Earth Surface Processes and Landforms, 16, pp. 427–445.

Carrara, A., Cardinali, M., Guzzetti, F. and Reichenbach, P., 1995, GIS-based techniques for mapping landslide hazard. *In: Geographical Information Systems in Assessing Natural Hazards*, Carrara, A. and Guzzetti, F. (Eds.), Kluwer Publications, Dordrecht, The Netherlands, pp. 135–176.

Carrara, A., Guzzetti, F., Cardinali, M. and Reichenbach, P., 1998, Current limitations in modeling landslide hazard, *In: Proceedings of IAMG'98*, Buccianti, A., Nardi, G. and Potenza, R. (Eds.), pp. 195–203.

Carrara, A., Guzzetti, F., Cardinali, M., and Reichenbach, P. 1999, Use of GIS Technology in the Prediction and Monitoring of Landslide Hazard, Natural Hazard, Kluwer Academic Publishers, 20, The Netherlands, pp.117–135.

Chacón, J., Irigaray, C., Fernández, T. and El Hamdouni, R., 2006, Engineering geology maps: landslides and geographical information systems. Bull. Eng. Geol. Environ., Springer-Verlag, 65, pp. 341–411.

Chung, C. F., Fabbri, A. G. and Van Westen C. J., 1995, Multivariate regression analysis for landslide hazard zonation, *In: Geographic Information Systems in Assessing Natural Hazards*, Carrara, A. and Guzzetti, F. (Eds.), Kluwer, Dordrecht, pp. 107–133.

Chung, C. F. and Fabbri, A. G., 2003, Validation of Spatial Prediction Models for Landslide Hazard Mapping, Natural Hazards, Kluwer Academic Publishers, 30, Netherlands, pp. 451–472.

Crozier, M. J., 1995, Landslide hazard assessment, theme report, *In*: *Landslides*, Bell (Ed.), Proceedings of the 6th International Symposium on Landslides, Balkema, Rotterdam, pp. 1843–1848.

Cruden, D. M. and Varnes, D. J., 1996, Landslide types and processes, *In: Landslides*, Schuster, R. L. and Turner, A. K. (Eds), investigation and mitigation, Transportation Research Board Special Report, National Academy Press, Washington, DC, v. 247, pp. 36–75.

Dhakal, A. S., Amada, T., and Aniya, M., 1999, Landslide hazard mapping and the application of GIS in the Kulekhani Watershed, Nepal, Mountain Research and Development, v. 19(1), pp. 3–16.

DHM, 1993, Climatological Records of Nepal, 1963-1993, Department of Hydrology and Meteorology (DHM), Ministry of Water Resources, Kathmandu, Nepal.

Esaki, T., Xie, M., Mitani, Y. and Zhou, G., 2004, Development of GIS-based spatial three-dimensional slope stability analysis system: 3DSlopeGIS, Jour. of Applied Computing in Civil Engineering, 13, pp 21–32.

Esaki, T., Thapa, P. B., Mitani, Y., and Ikemi, H., 2005, Landslide and Debris flow Characteristics and Hazard Mapping in Mountain Hill-slope Terrain by Using GIS, Central Nepal, *In*: *Landslide Risk Management*, Hungr, O., Fell, R., Couture, R., Eberhardt, E. (Eds.), Proceedings of the International Conference on Landslide Risk Management, Vancouver, Canada, A. A. Balkema, pp. 657–668.

Guzzetti, F., Carrarra, A., Cardinali, M., and Reichenbach P., 1999, Landslide hazard evaluation: A review of current techniques and their application in a multi-scale study, central Italy, Geomorphology, 31, pp. 181–216.

Hansen, A., 1984, Landslide hazard analysis, *In*: *Slope Instability*, Brunsden, D. and Prior, D. B. (Eds.), John Wiley and Sons, New York, pp. 523–602.

Hungr, O. 1995, A model for the runout analysis of rapid flow slides, debris flows and avalanches, Canadian Geotechnical Journal, v. 32(4) pp. 610–623.

Hungr, O., Evans, S. G., Bovis, M. and Hutchinson, J. N., 2001, Review of the classification of landslides of the flow type.

Hutchinson, J. N., 1988, General report: morphological and geotechnical parameters of landslides in relation to geology and hydrology, 5th International Symposium on Landslides, Lausanne, 1, pp. 3–35.

Luzi, L. and Pergalani, F., 1996, A methodology for slope instability zonation using a probabilistic method, Actas VI Congreso Nacional y Conferencia Internacional de Geología Ambiental y Ordenación del Territorio, 1, pp. 537–556.

Mark, R. K. and Ellen, S. D., 1995, Statistical and simulation models for mapping debris-flows hazard. *In: Geographical Information Systems in Assessing Natural Hazards*, Carrara, A. and Guzzetti, F. (Eds), Kluwer Academic Publisher, Dordrecht, The Netherlands pp. 93–106.

Montgomery, D. R. and Dietrich, W. E., 1994, A physically based model for the topographic control of shallow landsliding. Water Resources Research, v. 30(4), pp. 1153–1171.

Pachauri, A. K. and Pant, M., 1992, Landslide hazard mapping based on geological attributes, Engineering Geology, 32, pp. 81–100.

Remondo, J., González, A., De Terán, J. R. D., Cendrero, A., Fabbri, A. and Chung, C. F., 2003, Validation of Landslide Susceptibility Maps; Examples and Applications from a Case Study in Northern Spain, Natural Hazards, 30: Kluwer Academic Publishers, Netherlands, pp. 437–449.

Rowbotham, D. N. and Dudycha, D., 1998, GIS modelling of slope stability in Phewa Tal Watershed, Nepal, Geomorphology, v. 26, pp. 151–170.

Sarkar, S., Kanungo, D. P., and Mehotra, G. S., 1995, Landslide hazard zonation: a case study in Garhwal Himalaya, India, Mountain Research and Development, 15, pp. 301–309.

Soeters, R. and van Westen, C. J., 1996, Slope Instability Recognition, Analysis and Zonation, *In: Landslides, investigation and mitigation*, Turner, A. K. and Schuster, R. L. (Eds.), Transportation Research Board, National Research Council, Special Report 247: National Academy Press, Washington D.C., U.S.A, pp. 129–177.

SPSS, 1997, *SPSS advanced statistics 7.5*, SPSS, Chicago.

Stöcklin, J. and Bhattarai, K. D., 1977, Geology of Kathmandu Area and Central Mahabharat Range, Nepal Himalaya, Kathamdnu: HMG/UNDP Mineral Exploration Project, Technical Report, New York, 64 p. (Unpublished Report.).

Stöcklin, J., 1980, Geology of Nepal and its Regional Frame, Jour. Geol. Soc., London, 137, pp. 1–34.

Terlien, M. T. J., van Westen, C. J. and van Asch, T. W. J., 1995, Deterministic modeling in GIS based landslide hazard assessment, *In: Geographic Information Systems in Assessing Natural Hazards*, Carrara, A. and Guzzetti, F. (Eds.), Kluwer Academic Publishers, Dordrecht, The Netherlands, pp. 57–78.

Thapa, P. B. and Dhital, M. R., 2000, Landslides and debris flows of 19-21 July 1993 in the Agra Khola watershed of central Nepal. Jour. Nepal Geol. Soc., v. 21, pp. 5 -20.

Thapa, P. B., Esaki, T., and Mitani, Y., 2004, Landslides and debrisflows characteristics and hazard mapping in the natural hill-slope terrain by using GIS, 2nd International Workshop on Earth Science and Technology, Kyushu University, Fukuoka, Japan, pp. 63–71.

Thapa, P. B., 2005, *GIS-based Quantitative Hazard Modelling of Landslide and Debris Flow in the Mountainous Terrain of Central Nepal*, Ph. D. Thesis submitted to Faculty of Engineering, Kyushu University, Japan, 189 p., unpublished.

Thapa, P. B. and Esaki, T., 2006, Integration of Spatial Data Based on Map Overlays in GIS for Landslide Hazard Analysis: Agra Khola Watershed, Central Nepal, News Bulletin of Nepal Geological Society, v. 23, pp. 47–49.

van Westen, C. J., 1993, *GISSIZ: Training package for geographic information systems in slope instability zonation, Volume 1-Theory*, International Institute for Aerospace Survey and Earth Sciences (ITC), 15, 245 p.

van Westen, C. J., Rengers, N., Terlien, M. T. J. and Soeters, R., 1997, Prediction of the occurrence of slope instability phenomena through GIS-based hazard zonation, Geologische Rundschau, 86, pp. 404–414.

Varnes, D. J., 1978, Slope movements, type and processes, *In: Landslide Analysis and Control*, Schuster, R. L. and Krizek, R. J. (Eds.), Transportation Research Board, National

Academy Sciences, Washington, DC, Special report 176, pp.11–33.
Varnes, D. J., 1984, *Landslide Hazard Zonation: A Review of Principles and Practice*, UNESCO Press, Paris.
Yin, K. L. and Yan, T. Z., 1988, Statistical prediction models for slope instability of metamorphosed rocks, *In Proceedings of the 5th International Symposium on Landslides*, Lausanne, Bonnard, C. (Eds.), Switzerland, Rotterdam, The Netherlands, A. A. Balkema, 2, pp. 1269–1272.